

Pygmy Gamow-Teller resonance in the $N = 50$ region: New evidence from staggering of β -delayed neutron-emission probabilities

D. Verney,¹ D. Testov,^{1,2,*} F. Ibrahim,¹ Yu. Penionzhkevich,^{2,3} B. Roussi re,¹ V. Smirnov,² F. Didierjean,⁴ K. Flanagan,⁵ S. Franchoo,¹ E. Kuznetsova,² R. Li,^{1,†} B. Marsh,⁶ I. Matea,¹ H. Pai,⁷ E. Sokol,² I. Stefan,¹ and D. Suzuki^{1,‡}

¹*Institut de Physique Nucl aire, CNRS-IN2P3, Univ. Paris-Sud, Universit  Paris-Saclay, 91406 Orsay Cedex, France*

²*Joint Institute for Nuclear Research, Joliot-Curie 6, 141980 Dubna, Moscow region, Russia*

³*National Research Nuclear University, Kashirskoye Shosse 31, Moscow 115409, Russia*

⁴*Universit  de Strasbourg, CNRS, IPHC UMR 7178, F-67000 Strasbourg, France*

⁵*University of Manchester, Oxford Road, Manchester, M13 9PL, United Kingdom*

⁶*CERN, CH-1211 Geneva 23, Switzerland*

⁷*Nuclear Physics Division, Saha Institute of Nuclear Physics, 1/AF Bidhannagar, Kolkata 700 064, India*

(Received 20 March 2017; published 23 May 2017)

We report on the β -delayed neutron emission probability (P_{1n}) measurements of the $^{82,83,84}\text{Ga}$ ($N = 51, 52, 53$) precursors performed in one single experiment using the ^3He neutron-counter TETRA at the ALTO facility in Orsay. Altogether our results for the three $A = 82, 83$, and 84 Ga precursors point towards a sizable P_{1n} staggering in the $N = 50$ region, similar to the one already observed just after the $N = 28$ shell closure in the K isotopes chain, hinting at a similar mechanism. We will discuss the possible microscopic origin of this behavior, i.e., the existence in the light $N = 51$ isotones of low-lying components of the so called pygmy Gamow-Teller resonance, already well established at $Z = 36$, and persisting toward ^{79}Ni .

DOI: [10.1103/PhysRevC.95.054320](https://doi.org/10.1103/PhysRevC.95.054320)

I. INTRODUCTION

The possible existence of low-lying structures in the β -strength function above the neutron-separation energy (S_n) had given rise to—sometimes bitter—debates in the past (see, e.g., Refs. [1–4] and, in particular, the conclusion in Ref. [5]). However, the occurrence of structures in the tail of the Gamow-Teller giant resonance (GTGR), energetically accessible in the β decay of very neutron-rich nuclei, is now a long-well-established, widespread phenomenon (see Ref. [4] and references therein) and has been shown to have important consequences for r-process calculations [6]. The existence of low-lying satellites of the GTGR, thereafter interpreted as components of a pygmy Gamow-Teller resonance (GTPR), was in fact predicted quite early by Ikeda and Fujita as a natural consequence of the violation of the Wigner supermultiplet symmetry due to spin-dependent components of the nuclear interaction. A nice illustration of the underlying mechanism leading to the creation of the GTPR can be found, e.g., in Fig. 7 of Ref. [7].

One of the consequences of the existence of these structures, which has seldom been noticed, is the clear oscillation of

the β -delayed one-neutron emission probabilities (P_{1n}) just after a neutron shell closure for a given (odd- Z) chain of precursors. The P_{1n} value for a $[Z, N_m + 1]$ (N_m : the magic neutron number) precursor is obviously small because the emitter is a closed neutron shell nucleus and the P_{1n} value for a $[Z, N_m + 2]$ precursor much higher due to the closed-shell + one-neutron nature of the emitter. But the P_{1n} value can decrease significantly for the $[Z, N_m + 3]$ precursor while the $(Q_\beta - S_n)$ window still increases from $(N_m + 2)$ to $(N_m + 3)$.

This phenomenon clearly occurs in the $Z = 19$ chain after the $N = 28$ shell closure [8] as illustrated by Fig. 1. According to the authors of Ref. [8], the oscillation in opposition of phase of the emitters S_n curve and precursors P_{1n} curve is interpreted as due to allowed GT transitions to states belonging to a low-lying (≈ 5.5 MeV) shell-model configuration, that is to say a low-lying structure in the β -strength function (i.e., a component pertaining to the GTPR). In this physical picture, it is because of the natural oscillation of the S_n values (see Fig. 1), between the $[Z, (N_m, N_m + 1, N_m + 2)]$ emitters, probing this low-lying region of the β strength and its structures, that a sizable P_{1n} staggering is observed.

But this effect is most probably not restricted to this light-mass region. It could, for example, explain the systematic occurrence of irregularities (clear spikes), after each neutron-shell closure, in the effective density parameters of a *structureless* β -strength function, obtained after a global fit to the experimental P_{1n} values; see Fig. 1 in Ref. [13].

In a recent neutron-spectroscopy study of the $[Z = 31, (N_m = 50) + 2]$ precursor, ^{83}Ga , Madurga *et al.* [14] have clearly observed accumulations of β strength in specific excitation-energy regions of the ^{83}Ge emitter. According to the previous remarks, the Ga chain, beyond $N_m = 50$, should then be an excellent test case to investigate further the $(N_m + 1, 2, 3)$ P_{1n} -oscillation phenomenon. It would appear

*Present address: Dipartimento di Fisica e Astronomia and INFN, Sezione di Padova, Padova, Italy.

†Present address: TRIUMF, 4004 Wesbrook Mall, Vancouver, British Columbia, Canada V6T2A3.

‡Present address: RIKEN Nishina Center, 2-1 Hirosawa, Wako, Saitama, 351-0198 Japan.

Published by the American Physical Society under the terms of the [Creative Commons Attribution 4.0 International](https://creativecommons.org/licenses/by/4.0/) license. Further distribution of this work must maintain attribution to the author(s) and the published article's title, journal citation, and DOI.

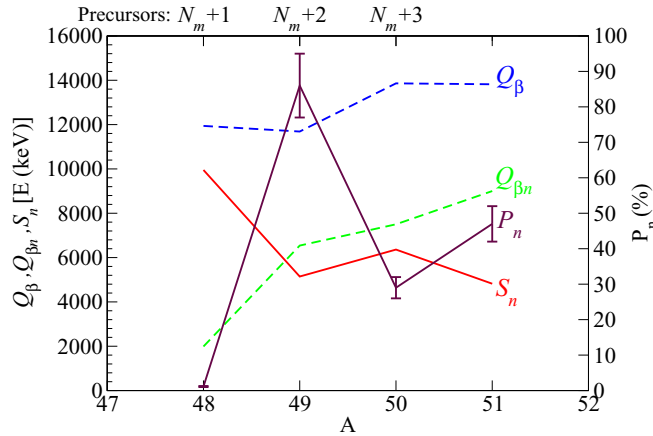


FIG. 1. Illustration of the $(N_m + 1, 2, 3)$ P_{1n} -oscillation phenomenon for the K ($Z = 19$) precursors beyond $N_m = 28$ using the Q_{β} and $Q_{\beta n}$ values of the $^{48-51}\text{K}$ precursors and S_n values of the $^{48-51}\text{Ca}$ emitters (left vertical axis), and P_{1n} values of the $^{48-51}\text{K}$ precursors (right vertical axis). All values are taken from Refs. [9–12].

at first sight that this phenomenon is absent from the Ga chain when considering, Fig. 2, the previous (somewhat discrepant) P_{1n} values accumulated for the $^{83,84}\text{Ga}$ precursors, which were obtained using various counting techniques. While overall these previous results point towards a trivial, regular increase of the P_{1n} values from the $(N_m + 1)$ to the $(N_m + 3)$ precursor, on the contrary, the most recent results from Ref. [14] interestingly suggest for the first time a P_{1n} -slope inversion at $(N_m + 2)$. We felt then that further investigation of the question could be in order.

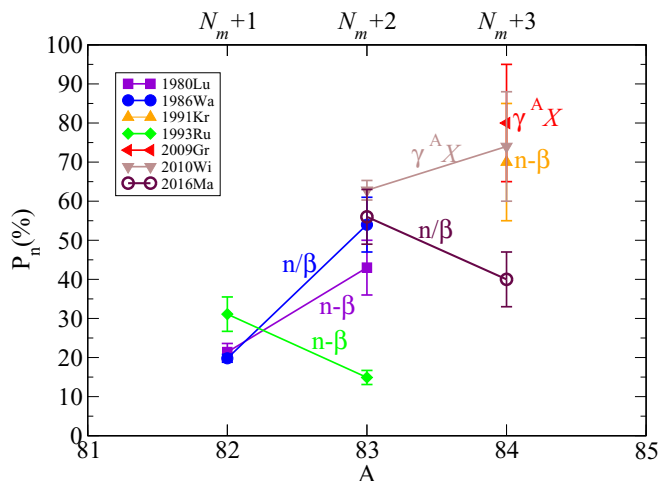


FIG. 2. Experimental P_{1n} values for the $^{82-84}\text{Ga}$ precursors available in literature: 1980Lu [15], 1986Wa [16], 1991Kr [17], 1993Ru [18], 2009Gr [19], 2010Wi [20], and 2016Ma [14]. The counting techniques employed are shown near the corresponding plots using the codes introduced in Ref. [18]: n/β for neutron- β coincidence technique, $n-\beta$ for simultaneous neutron and β counting, and $\gamma ^A X$ when the remaining abundance of the emitter after neutron emission was determined by γ counting of a daughter.

We report in this paper on the P_{1n} measurements of the $^{82,83,84}\text{Ga}$ ($N = 51, 52, 53$) precursors performed in one single experiment using the ^3He neutron-counter TETRA [21,22] at the ALTO facility in Orsay [23]. Our results for ^{82}Ga were already reported in Ref. [22]. Since it is for this precursor that the best agreement between P_{1n} values obtained from different counting techniques was previously found (see Fig. 2), it was used as a test case to validate our experimental procedure. Consequently, the experimental details and analysis procedure will be only briefly reviewed in Sec. II; they have been already presented and extensively discussed in Ref. [22]. However, we provide details about further improvements of our analysis procedure introduced to demonstrate the reliability of the P_{1n} measurement for the ^{83}Ga precursor. The results from this experiment for both the $A = 83$ and 84 Ga precursors will be presented in Sec. III. In particular, we make detailed β -neutron doubly gated γ -spectroscopy data on $^{83,84}\text{Ge}$ available for the first time in literature. Altogether, our results for the three $A = 82, 83$, and 84 Ga isotopes point toward a strong P_{1n} staggering in the $N = 50$ region, similar to the one already known in the $N = 28$ region, hinting at a similar mechanism. For that reason, this result is discussed in Sec. IV, highlighting the possible microscopic origin of this behavior, i.e., the existence in the $N = 50$ region of a low-lying component of the GTPR, well established at $Z = 36$ and persisting toward ^{78}Ni .

II. EXPERIMENTAL DETAILS AND DATA ANALYSIS

A. Experimental details

All details concerning this experiment from the experimental arrangement to the chosen methodology for the extraction of P_{1n} values can be found in Ref. [22] and we only recall here briefly some of the most relevant aspects for the present article.

Selectively laser-ionized Ga beams were collected onto an Al-coated Mylar movable tape at the geometrical center of the ^3He neutron-counter TETRA. The collection point was surrounded by a plastic scintillator for β detection. A coaxial HPGe detector (EUROGAM-1) was used for γ detection. The counting cycles were divided in three phases. A short beam-off counting time T_{bg} was allowed before each beam collection to measure the background level and to monitor possible activity build-in off the tape. After a beam collection of T_{coll} duration, the beam was deflected and the decay of the source counted for T_{dec} . Then the tape was moved for 2 m to transport the source outside the detection array. The time parameters $T_{\text{bg, coll, dec}}$ and the number of cycle repetitions N_{cycles} for the $A = 82, 83, 84$ measurements are summarized in Table I.

B. P_{1n} extraction procedure

As explained in Ref. [22], the β -delayed one-neutron emission probability P_{1n} and beam rate ϕ (pps) were determined from the observed grow-in/decay β and neutron activity curves, cumulated over N_{cycles} , by solving the corresponding Bateman equation system. Once P_{1n} and ϕ are determined, the individual contributions to the total observed β -activity curves, stemming from the β activities of the mother and all

TABLE I. Tape-cycle parameters used for the $A = 82, 83, 84$ settings: T_{bg} is the background counting time before beam collection, T_{coll} is the duration of the beam collection, and T_{dec} is the beam-off source decay counting time, in ms. N_{cycles} is the total number of tape cycles for each mass setting.

Beam	T_{bg}	T_{coll}	T_{dec}	N_{cycles}
^{82}Ga	100	2000	0	1700
^{83}Ga	100	3000	2000	4405
^{84}Ga	500	3000	500	17971

possible β and β - n daughter nuclei, were determined. This information was used as a consistency test.

A constant *average* beam rate ϕ over N_{cycles} was assumed for a given mass setting based on the fact that, due to the primary electron beam microstructure, the radioactive ion beam at ALTO is continuous in nature. Strictly speaking, ϕ is not really independent of time during the measurement because of the inevitable slow modification of target-ion-source conditions under continuous heating and irradiation. But this cannot modify the collection curve shapes unless the radioactive ion beam has a time structure (i) varying strongly within T_{coll} and (ii) varying *periodically* with a period of the order of the tape cycle *and* in phase with it. These two conditions are simply not met: The observed variations of the beam intensity at ALTO are slow, with characteristic times of the order of tens of minutes, and random in nature. The fact that the correct precursor half-life can be obtained from the neutron activity curves restricted to the grow-in part, as shown in Ref. [22], further supports this assumption. However, for this present article we have decided to further investigate this question.

C. Cycle-per-cycle analysis

In Ref. [22], the total cumulated neutron and β activities were analyzed using the corresponding Bateman equation system. In the present work, in order to achieve a quantitative

evaluation of the beam fluctuations and to understand their influence on the obtained P_{1n} values, the Bateman equation system was solved for the β and neutron activity curves obtained for each individual cycle of the $A = 83$ setting. An example of single-cycle analysis is illustrated by Fig. 3. Two distributions of $N_{cycles} = 4405$ values, for P_{1n} and ϕ , were then obtained, which are reported in Fig. 4.

The distribution of the P_{1n} values can be fitted by a Gaussian function, the corresponding mean value of the distribution is $\bar{P}_{1n}(^{83}\text{Ga}) = 0.850(2)$. Inclusion of the statistical errors determined for each individual cycle allows obtaining two shifted distributions representing the maximum and minimum values within $\approx 1\sigma$ statistical uncertainties, which are represented by the hatched histograms in Fig. 4. This leads to a range of $\bar{P}_{1n}(^{83}\text{Ga})$ possible values given by $0.824(2) \leq \bar{P}_{1n}(^{83}\text{Ga}) \leq 0.878(2)$. The $\bar{P}_{1n}(^{83}\text{Ga})$ range reflects both statistical uncertainties and part of the systematic uncertainties associated to beam fluctuations. The other sources of systematic uncertainties originate from the β and neutron-detection efficiency (ϵ_β and ϵ_n) determination. As in Ref. [22], these detection efficiencies were determined from the observed ratios of peak areas in singles, β and β - n gated γ spectra (see Ref. [22] for more details). The adopted ϵ_β , ϵ_n values and associated uncertainties are summarized in Table II. Some of the ratios used to obtain these adopted values are reported in Tables IV and VI of Sec. III, when possible. In the case of ^{84}Ga , due to the very low production yield, peaks were difficult to exploit in the singles spectra. For that reason, $\epsilon_\beta^{(84)} \approx \epsilon_\beta^{(83)}$ was assumed.

The result from the total cumulated curve analysis, as shown in Fig. 5 of Sec. III, leads to $P_{1n}(^{83}\text{Ga}) = 85(4)\%$. This value is quite consistent with the observed \bar{P}_{1n} range, being located exactly at the range midvalue, and the associated uncertainty is also consistent with the range width. This definitely proves that—within the specific experimental conditions found at ALTO—the assumption of an average constant beam rate over the full number of tape cycles for a given mass setting is correct.

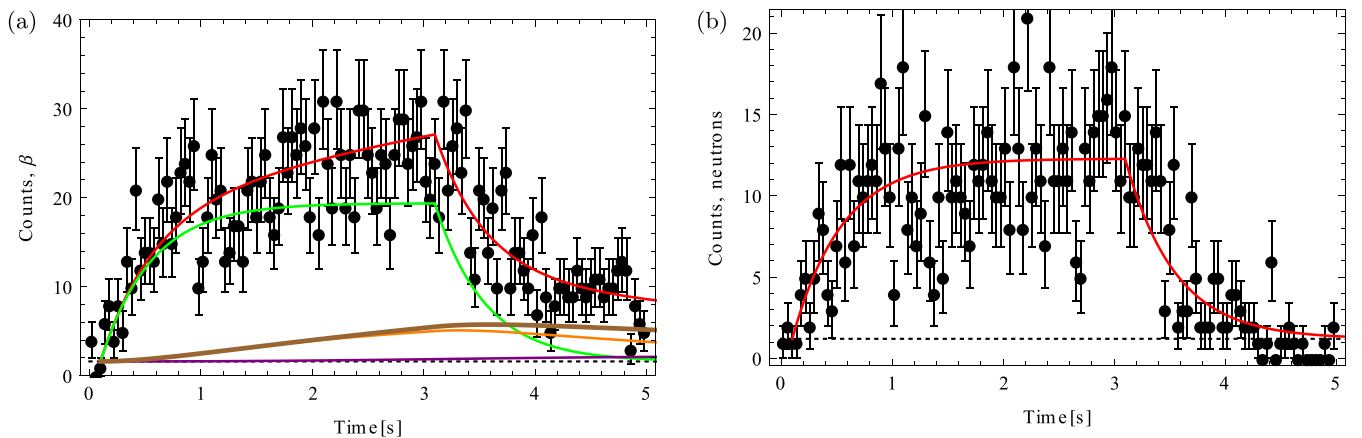


FIG. 3. Example of β (a) and neutron (b) activity curves (black dots) for a 3-s-long ^{83}Ga -beam collection followed by a 2-s-long decay within a single tape cycle. In panel (a), the individual components of the total β activity (red curve) are shown by different colored curves, ^{83}Ga in green, ^{83}Ge in orange, ^{83}As in purple, and ^{82}Ge in brown, and the background is shown by the dashed line.

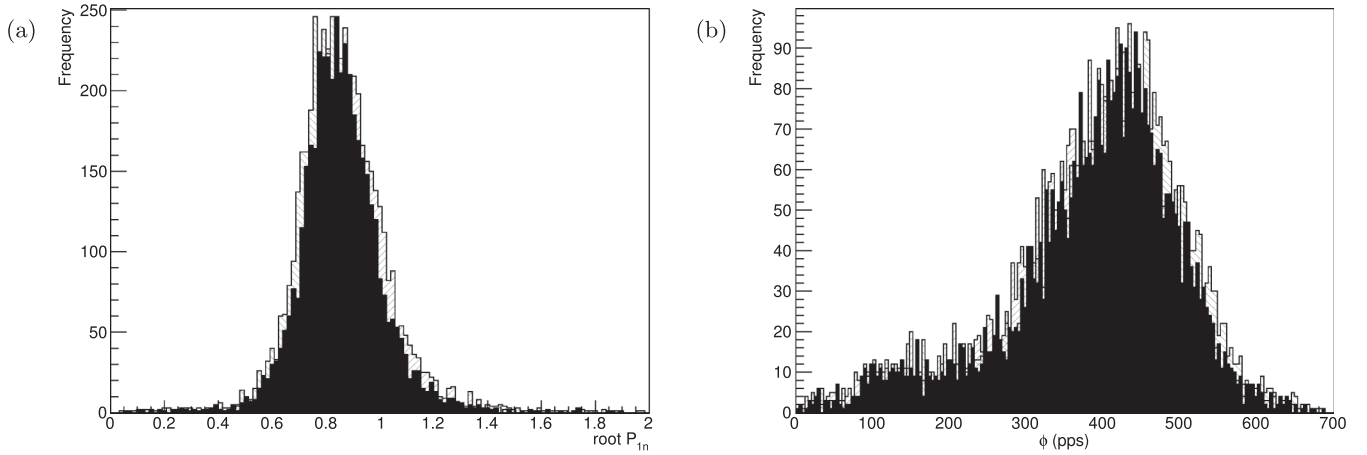


FIG. 4. Distributions of the P_{1n} (a) and ϕ (b) values extracted from each of the 4405 cycles of the $A = 83$ setting measurement. The hatched histograms correspond to the higher and lower limits considering the statistical uncertainties for each cycle.

The beam intensity distribution in Fig. 4 can readily be interpreted as representing the beam fluctuations. It is seen in particular that despite the presence of a low-intensity tail, the beam was quite stable with an average beam rate around 400 pps. It is worth, for the rest of the discussion, to recall here that usually a reliable ion counting is difficult to obtain with movable-tape collector-based techniques due to the very low energy of the beam and its interception by the tape. The simultaneous registration of the β and neutron curves actually provides a robust working method for obtaining ion counting independently from any prior knowledge of the γ branching ratios in the decay chain. However, it should be noted that this method entirely relies on (i) a reliable set of half-life values for all the decay daughters and (ii) the correct determination of the β - and neutron-detection efficiencies.

III. RESULTS

A. ^{83}Ga decay

1. Results from the cumulated activity curves

The cumulated β and neutron curves obtained for $A = 83$ are shown in Fig. 5. All neutrons detected for the $A = 83$ setting were attributed either to the background or to the ^{83}Ga β - n decay: β -delayed neutron emission is indeed less energetically possible for the higher- Z $A = 83$ isobars and has not been reported so far. The fit to the grow-in and decay

TABLE II. β and neutron detection efficiency values, ϵ_β and ϵ_n , used for the analysis. The efficiencies are obtained from the observed ratios of peak areas in singles, β , and β - n gated γ spectra.

Beam	ϵ_β (%)	ϵ_n (%)
^{82}Ga	63(4)	63(6)
^{83}Ga	62(4)	59(5)
^{84}Ga	62(4) ^a	57(5)

^aAssumed equal to the value for $A = 83$; see text.

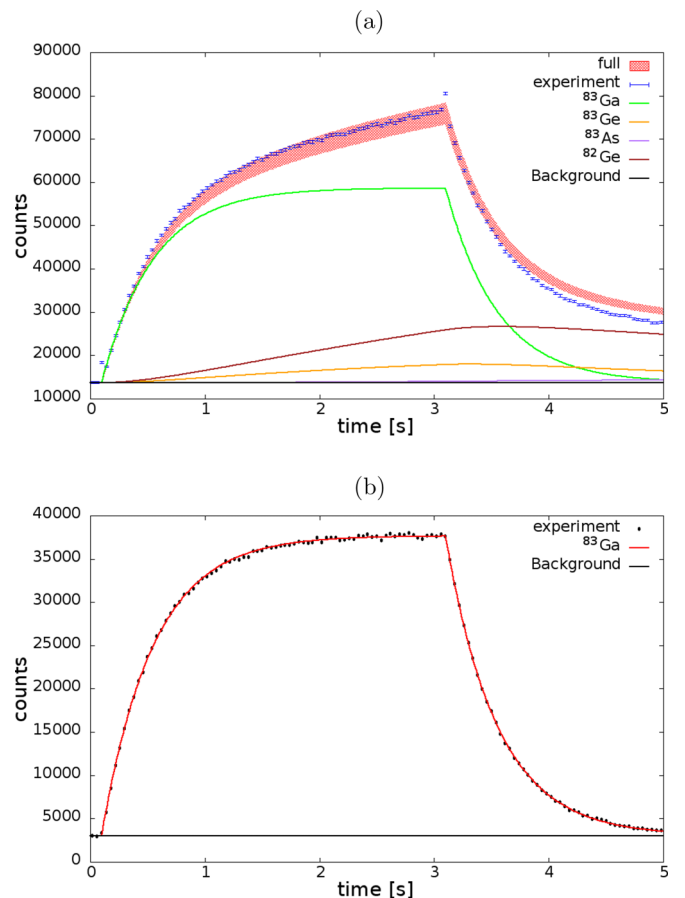


FIG. 5. β (a) and neutron (b) activity curves (dots) recorded for the $A = 83$ setting of the mass separator. These curves were accumulated over 4405 tape cycles. (a) The different β -activity components are singled out with colored curves. (b) The neutron activity is attributed solely to the ^{83}Ga β - n decay. This activity curve is then characterized by the half-life of the ^{83}Ga precursor. The result from the fit to the neutron activity curve is $T_{1/2} = 0.312(1)$ s (red curve).

TABLE III. Summary of the results obtained from the analysis of the cumulated β - and neutron-activity curves for the $A = 82, 83, 84$ settings.

Precursor	Beam rate ϕ (pps)	P_{1n} (%)	$T_{1/2}$ (ms)
^{82}Ga	1290(60)	22(2)	604(11)
^{83}Ga	370(20)	85(4)	312(1)
^{84}Ga	5(2)	53(20)	

patterns of the cumulated neutron activity curve, as shown in Fig. 5, leads to a ^{83}Ga half-life value of 0.312(1) s, where the uncertainty is the uncertainty from the fit. This value is compatible within error bars with all previous measurements (see Refs. [24,25]) with the exception of the one at 308(1) ms from Ref. [17] (but very close to it).

As explained earlier ϕ and P_{1n} are determined by solving the Bateman equation system associated to the β - and neutron-activity curves, we obtain $\phi = 370(20)$ pps and $P_n = 85(4)\%$ (all the results are summarized in Table III). As can be seen in Fig. 2, this value is larger than any of the previously reported ones. This confirms the fact, first discovered by Winger *et al.* [20], that ^{83}Ge is a much stronger β -delayed neutron emitter than thought before and that the β - n channel dominates by far the ^{83}Ga decay. As far as we can understand, the reported $P_{1n} = 62.8(25)\%$ value obtained in Ref. [20] relied on the ^{82}Ge population estimation from γ counting, based on an unspecified branching ratio to the 1092-keV transition in ^{82}As . In the very recent work by Madurga *et al.* [14], an even lower value ($P_{1n} = 56(7)\%$) was obtained from an integral of the neutron spectrum. This spectrum shows that the neutron energy spectrum is peaked around 2 MeV and extends below this energy. This is the energy regime where the detection efficiency can be directly measured with TETRA using a ^{252}Cf source [22]; i.e., it is well under control. Our measurement is based on the robust simultaneous, individual β , and neutron counting with 4π detectors, and, thanks to the cycle-per-cycle analysis procedure, is statistically highly significant. A possible explanation for the possibly missing ($\approx 30\%$) β -delayed neutron strength in Ref. [14] could be that a significant fraction of the neutrons are emitted at very low energy (possibly below the claimed 70-keV energy threshold in this reference). This hypothesis would be consistent with the microscopic origin of the P_{1n} staggering as will be tentatively explained in Sec. IV.

Once ϕ , $T_{1/2}$, and P_{1n} for the precursor are determined, one can restore the expected total β -activity curve as well as the individual β contributions to it due to the precursor itself and its daughters' activities, using the tabulated daughter half-life values, as consistency test. Including the uncertainties, one obtains the red region as shown in the top panel of Fig. 5. This curve is in good agreement with the measured one. However, one sees that the measured activity is somewhat lower than the calculated one near the end of the decay part of the cycles. A perfect reproduction can be obtained if, for instance, one uses a longer half-life value for ^{82}Ge of $\simeq 8$ s, instead of the recommended value of 4.55(5) s [26]. This might indicate the presence of a weak, unidentified long-lived β -activity

component, maybe an unidentified β -decaying isomer in one of the nuclides in the decay chain.

2. βn -gated γ spectroscopy

We present in Fig. 6 the β and β - n gated γ spectra obtained for the $A = 83$ setting of the mass separator. Practically all the observed lines could be attributed to the β and β - n decays of the collected ^{83}Ga beam and its daughter chains (with the exception of two obviously visible lines in the 2800- to 2900-keV region). This proves that the beam was indeed quite pure. The energies and relative intensities of the γ transitions which could be attributed to the β and β - n channels of the ^{83}Ga decay from these spectra are reported in Table IV. The branching ratios to the $^{82,83}\text{Ge}$ levels and absolute γ intensities were obtained using the ion-counting method described previously, i.e., without the need of any γ -branching ratios to As daughters. Transitions placements from previous works (see first column in Table IV) were used to deduce the β and β - n branching ratios. All the lines previously attributed to the β - n decay of ^{83}Ga by Winger *et al.* [20] could be confirmed. We could also confirm some of the transitions in ^{82}Ge observed in additional spontaneous-fission and ^{82}Ga β -decay studies [25,27]. A set of previously unreported lines and their proposed assignment is listed in Table V. Strict criteria were used to propose these new γ rays. Assignment to the ^{83}Ga β - n decay is made only if the three following conditions are fulfilled: (i) the net count S (above background) in the peak region in both β and β - n gated spectra ($S_{\gamma\beta}$ and $S_{\gamma\beta n}$ respectively) is above the critical limit (see Ref. [28,29] for a proper definition) for 95% confidence; (ii) the ratio $S_{\gamma\beta n}/S_{\gamma\beta}$ is compatible with the measured neutron-detection efficiency (ϵ_n in Table II), and (iii) the relative uncertainty $\Delta S/S \lesssim 0.75$. We decided to assign new γ rays to the ^{83}Ga β -channel only if they were also unambiguously observed in the ^{84}Ga β - n channel (see following subsection). In the end, only the line at 1795.1 keV passed this test; the other unidentified peaks were left unassigned and marked by ? in Fig. 6.

We also note energy-unresolved excesses of counts in the β - n gated spectra in the region above 600 keV and in the one centered around 844 keV. The former, with a typical triangular shape, is easily explained by inelastic neutron scattering on Ge nuclei of the detector's crystal subsequently detected by TETRA, leading to spurious γ - n coincidences. The latter is most probably due to neutron inelastic scattering on ^{56}Fe , though the presence of iron in our setup should be extremely marginal. This may also explain the slight excess of counts observed at 1238 keV in the β - n gated spectrum while the 1238 keV unambiguously belongs to the ^{83}Ge level scheme. At last, the peak observed in the β - n gated γ spectrum at 1092 keV, which is the main γ line in the ^{82}Ge decay to ^{82}As , is due to random γ - n coincidences. Its intensity is $\approx 2\%$ of the corresponding one in the β -gated spectrum, a value consistent with a 128- μs opening of the γ - n coincidence window [30].

The observed γ -intensities relative to 1348-keV transition are, on the overall, in fair agreement with those reported in Ref. [20]. However, one should note the large difference of the dominant β - n branching ratio, to the 2^+_{1} ^{82}Ge excited state, which is of 45(11)% in our case *vs* 19.6(8)% in Ref. [20]. In

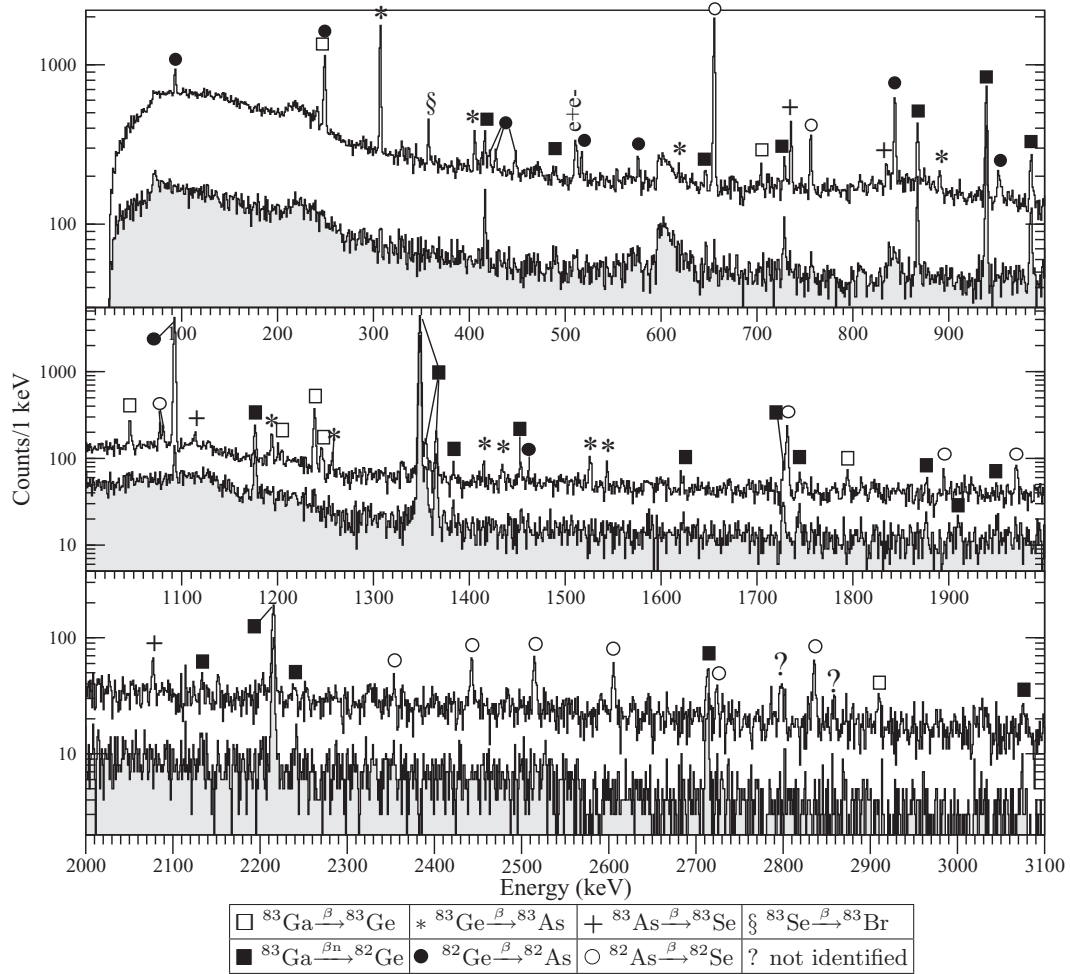


FIG. 6. β gated and β - n gated (shaded in gray) γ spectra recorded for the $A = 83$ setting of the mass separator.

the present case, the uncertainties on the absolute quantities are large (and probably somewhat conservative). They reflect the uncertainty of the calibration source positioning in a very closed geometry where even an error of the order of ≈ 1 mm can result in significant change in the measured absolute efficiency. Nevertheless, we note that we found a similar ($\approx 45\%$) value in the more recent measurements at ALTO, reported in Refs. [35,36], where γ - γ coincidence relationships could be established and transitions placements were possible.

B. ^{84}Ga decay

1. Results from the cumulated activity curves

The β and neutron activity curves cumulated over 17 971 tape cycles are presented in Fig. 7. In the case of the $A = 84$ measurement, neutrons observed have two possible origins, one from the decay of ^{84}Ga and the other from the decay of its daughter ^{84}Ge . The neutron contribution from the last was determined using the recommended value of $P_{1n}(^{84}\text{Ge}) = 10.2(9)$ [37]. As can be seen in Fig. 7, thanks to the large

difference between the two neutron precursors' half-lives and the chosen tape cycling (see Table I), the neutron contribution from the ^{84}Ge decay remained marginal.

From Table III, one can immediately point out that the measured production rate for ^{84}Ga was lower by two orders of magnitude with respect to the one for ^{83}Ga . This ^{84}Ga production yield of 5(2) pps only is to be compared to the one of ≈ 120 pps obtained in our previous experiment using laser ionization for Ga with similar electron primary beam intensity and target mass [38]. This reflects the progressive degradation of the laser ion-source conditions that was observed during the present experiment (the $A = 84$ measurement was the last of the experiment).

Despite a longer counting time devoted to the $A = 84$ setting (see the different N_{cycles} values in Table I), the collected statistics remained limited and cycle-per-cycle analysis technique could not be used. With the standard method of Ref. [22] we obtain $P_{1n} = 53(20)\%$ for the ^{84}Ga β -delayed neutron emission probability, assuming emission of one single neutron (two neutron emission is likely, see later, but the effect is meaningless within our large error bars). With this value,

TABLE IV. Photopeaks attributed to the β and β - n decays of ^{83}Ga identified in the spectra recorded for the $A = 83$ setting of the mass separator. γ intensities are given relative to the one of the transition observed at 1348 keV. In the fourth column (Spec) are specified the γ spectra of Fig. 6 which were used to determine the different quantities, labeled $\gamma\beta$ and $\gamma\beta n$ for the singly β -gated and doubly β -neutron gated γ spectra respectively. Following the methodology introduced in Ref. [22], $S_{\gamma\beta}/S_{\gamma}$ and $S_{\gamma\beta n}/S_{\gamma\beta}$ are the quantities used to determine the β and neutron effective detection efficiencies reported in Table II. Placements in the daughter level schemes are from references quoted in the first column. Bracketed γ energies correspond to transitions observed elsewhere but not in the present work. Direct β -branching ratios (I_{β}) to the levels quoted in the first column are *apparent* branching ratios based only on the γ transitions observed in the present work.

E_{level} [keV] (daughter)	I_{β} [%]	E_{γ} [keV]	Spec	I_{γ}^{rel} [%]	$S_{\gamma\beta}/S_{\gamma}$ [%]	$S_{\gamma\beta n}/S_{\gamma\beta}$ [%]
$^{83}\text{Ga} \xrightarrow{\beta-n} ^{82}\text{Ge}$						
1348.08[20]	45(11)	1348.5(8)	$\gamma\beta$	100.0(13)	68(1)	
		1348.5(8)	$\gamma\beta n$	100.0(16)		60(1)
2214.91 [20]	6.6(13)	867.6(5)	$\gamma\beta$	3.8(4)		
		867.4(5)	$\gamma\beta n$	3.2(3)		59(13)
		2215.2(4)	$\gamma\beta$	7.7(15)		
		2215.2(4)	$\gamma\beta n$	8.5(8)		66(5)
2286.87 [20]	5.4(13)	939.2(5)	$\gamma\beta$	11.4(4)	59(4)	
		939.3(5)	$\gamma\beta n$	11.3(4)		56(3)
2333.2 [20]	1.7(4)	985.7(5)	$\gamma\beta$	2.7(4)		
		985.9(5)	$\gamma\beta n$	2.4(3)		52(7)
2524.19 [20]	2.0(5)	(191.4 [27])				
		1176.7(5)	$\gamma\beta$	3.3(5)		
		1176.8(5)	$\gamma\beta n$	2.9(4)		52(7)
		(2524.7 [27])				
2702.27 [20]	1.8(4)	416.4(4)	$\gamma\beta$	1.0(2)		
		416.4(4)	$\gamma\beta n$	1.0(2)		57(23)
		487.0(5) ^a	$\gamma\beta$	0.3(2)		
		487.6(5)	$\gamma\beta n$	0.2(1)		57(34)
		1354.4(4)	$\gamma\beta$	1.9(4)		
		1354.3(4)	$\gamma\beta n$	1.7(4)		47(18)
2713.5 [20]	3.6(10)	1365.5(4)	$\gamma\beta$	3.6(6)	62(7)	
		1365.4(4)	$\gamma\beta n$	3.7(4)		62(7)
		2713.4(5)	$\gamma\beta$	2.2(6)		
		2713.1(5)	$\gamma\beta n$	2.3(4)		66(13)
2883.28 [20]		(596.4 [20]) ^b	$\gamma\beta$			
2933.0 [27]	0.3(1)	646.3(5)	$\gamma\beta$	0.4(2)		
		646.8(5)	$\gamma\beta n$	0.6(3)		48(23)
3014.5 [20]	0.8(3)	728.8(6)	$\gamma\beta$	1.3(2)		
		728.6(6)	$\gamma\beta n$	1.1(4)		58(23)
3076.3 [25]	1.1(3)	1728.0(4)	$\gamma\beta$	1.2(3)		
		1727.6(4)	$\gamma\beta n$	1.4(2)		73(17)
		3076.0(6)	$\gamma\beta$	0.6(4)		
		3076.0(5)	$\gamma\beta n$	0.6(4)		
3257.4 [27,32]	0.2(2)	(201.9 [27])				
		1908.8(2) ^c	$\gamma\beta$	0.4(3)		
		1908.4(4)	$\gamma\beta n$	0.3(3)		60(37)
		(3257.4 [27])				
Remaining ^d (γ unobserved)	20(8)		$\gamma\beta n$			
$^{83}\text{Ga} \xrightarrow{\beta-} ^{83}\text{Ge}$						
247.05 [20]	$\lesssim 0.5$	249.2(5) ^e	$\gamma\beta$	$\lesssim 1.6$	57(5)	
1045.5[20]	2.2(5)	(798.9[25,38])	$\gamma\beta$			
		1045.0(3)	$\gamma\beta$	3.3(8)	61(15)	
1238.0[20]	4.0(10)	1238.6(5)	$\gamma\beta$	7.2(3)	67(8)	
1245.7[25]	1.0(3)	1245.6(2)	$\gamma\beta$	1.7(3)		
1452.7[38]	0.5(1)	1204.4(4)	$\gamma\beta$	0.8(3)		

TABLE IV. (*Continued*).

E_{level} [keV] (daughter)	I_{β} [%]	E_{γ} [keV]	Spec	I_{γ}^{rel} [%]	$S_{\gamma\beta n}/S_{\gamma\beta}$ [%]	$S_{\gamma\beta n}/S_{\gamma\beta}$ [%]
1941.2[25]	0.4(1)	704.3(8)	$\gamma\beta$	0.7(2)		
Remaining (γ unobserved)	$\leq 12.9^{\text{f}}$		$\gamma\beta$			

^aWeak line, but the net count is above the critical limit for 95% confidence. A transition at 487.0 keV depopulating the level at 2702.1 keV was observed in the β decay of ^{82}Ga in Ref. [31] (placement is uncertain).

^bThis line is probably present in our spectra too. But its close proximity to the $^{74}\text{Ge}(n,n')$ prevents any quantitative determination of the peak surface both in β -gated and β - n -gated spectra.

^cWeak line, the net count is at the critical limit for 95% confidence, it might correspond to the 1908.9-keV line reported in Ref. [27].

^dTo be considered only as an upper limit for the direct β - n branching to the ^{82}Ge ground state.

^eThe time behavior in the collection-decay cycles for this line is characteristic of a mixture with the 249.1-keV line observed in the decay of ^{82}Ge [33,34]. I_{γ}^{rel} was obtained from the analysis of these curves assuming two time components.

^fWe report $I_{\beta} = 16(4)\%$ to (neutron-unbound) levels in the 4-9 MeV energy region in a separate article [35] (this result was obtained from a measurement dedicated to β -delayed high-energy γ emissions from ^{83}Ge at ALTO). Consequently the direct β -branching ratio to the ^{83}Ge ground state must be close to zero.

we confirm a significant decrease of the P_{1n} value from ^{83}Ga to ^{84}Ga recently hinted at in Ref. [14].

The fit to the neutron curve (Fig. 7) looks less satisfactory than in the ^{83}Ga case, but the integral of the neutron counts is quite stable against parameter changes, so is the resulting P_{1n} . The origin of the uncertainty on this P_{1n} value is in fact mainly of statistical nature. The fit shown in Fig. 7 was done assuming $T_{1/2}(^{84}\text{Ga}) = 84(7)$ ms. This value is obtained as the

weighted average of all the half-lives from the γ -ray decay curves reported in Table I of Ref. [38] (the currently adopted value is 85(10) ms [37] originating from Ref. [17]).

2. β - n -gated γ -spectroscopy

The β and doubly β - n gated γ spectra recorded at the $A = 84$ mass-separator setting are shown in Fig. 8. Due to insufficient statistics, only the strongest lines observed from the ^{84}Ga decay in Ref. [38] were visible (see Table VI). No transition with an intensity lower than 10% of the strongest 248 keV one could be observed. The relative intensities of the strongest lines reported in Table VI are in good agreement with those from Ref. [38]. It seems, however, that we somewhat overestimate those of the weaker lines, which appear as small peaks, resulting in large I_{γ} uncertainties.

Despite ungrateful data, two interesting findings may worth being pointed out. First, we clearly observe a peak at 307 keV in the doubly β - n -gated γ spectrum (marked with the symbol ♣ in Fig. 7). It is the strongest γ line known in the β decay of ^{83}Ge [24] and is indeed clearly visible in the β -gated γ spectrum. However, the obtained ratio $S_{\gamma\beta n}/S_{\gamma\beta} = 10(3)$ is at the same time far above the expected level of 2% for random γ - n coincidence (see previous subsection) and far below the 57(5)% neutron efficiency. This is easily explained by the fact that the 307-keV line in the β -gated spectrum contains two contributions, one from the β channel of the ^{83}Ge decay, and the other from the β - n channel of the ^{84}Ge decay. While in the doubly β - n -gated spectrum only one of the two components is present. This confirms the assignment of the 307-keV γ ray to the βn decay of ^{84}Ge recently reported in Ref. [39].

Second, one can notice an accumulation of statistics in the 1348-keV energy region (corresponding to the $2^+_{11} \rightarrow 0^+_{\text{gs}}$ transition in ^{82}Ge) of the β - n -gated spectrum, marked with a ♦ symbol in Fig. 8, and actually forming a peak. The net count in this peak above the (low) background of the β - n -gated spectrum is above the critical limit for 95% confidence. However the estimation of the corresponding peak surface in the singly β -gated γ spectrum is very difficult. This peak was also visible in the spectra of Ref. [38] but not assigned in this reference. It

TABLE V. Previously unreported photopeaks observed in the spectra recorded for the $A = 83$ setting of the mass separator. Second column (Spec): γ spectra of Fig. 6 where the peaks were observed ($\gamma\beta$ and $\gamma\beta n$ for the singly β -gated and doubly β -neutron gated γ spectra respectively). I_{γ}^{rel} : intensities relative to the transition observed at 1348.5 keV (n.o., not observed). Forth column: ratios of peak areas measured in the β -neutron gated and β -gated γ spectra to verify the consistency with the measured neutron efficiency. No placement is proposed for these transitions.

E_{γ} [keV]	Spec	I_{γ}^{rel} [%]	$S_{\gamma\beta n}/S_{\gamma\beta}$ [%]	Assignment
1383.7(5)	$\gamma\beta$	0.7(2)		$^{83}\text{Ga}(\beta n)$
	$\gamma\beta n$	0.6(2)	51(23)	
1454.0(5)	$\gamma\beta$	1.6(3)		$^{83}\text{Ga}(\beta n)$
	$\gamma\beta n$	1.3(3)	47(13)	
1622.0(3)	$\gamma\beta$	1.0(3)		$^{83}\text{Ga}(\beta n)$
	$\gamma\beta n$	0.8(3)	48(20)	
1744.5(4)	$\gamma\beta$	0.9(3)		$^{83}\text{Ga}(\beta n)$
	$\gamma\beta n$	0.9(3)	61(38)	
1795.1(4)	$\gamma\beta$	1.7(3)		$^{83}\text{Ga}(\beta)^{\text{a}}$
	$\gamma\beta n$	n.o.		
1876.1(6)	$\gamma\beta$	1.1(3)		$^{83}\text{Ga}(\beta n)$
	$\gamma\beta n$	0.5(1)	52(22)	
2134.0(5)	$\gamma\beta$	0.9(3)		$^{83}\text{Ga}(\beta n)$
	$\gamma\beta n$	0.6(3) ^b	33(19) ^b	

^aTransition also observed in the β - n -gated γ spectra recorded at $A = 84$; see Table VI.

^bWeak line in the β - n -gated spectra; the net count is just at the critical limit for 95% confidence.

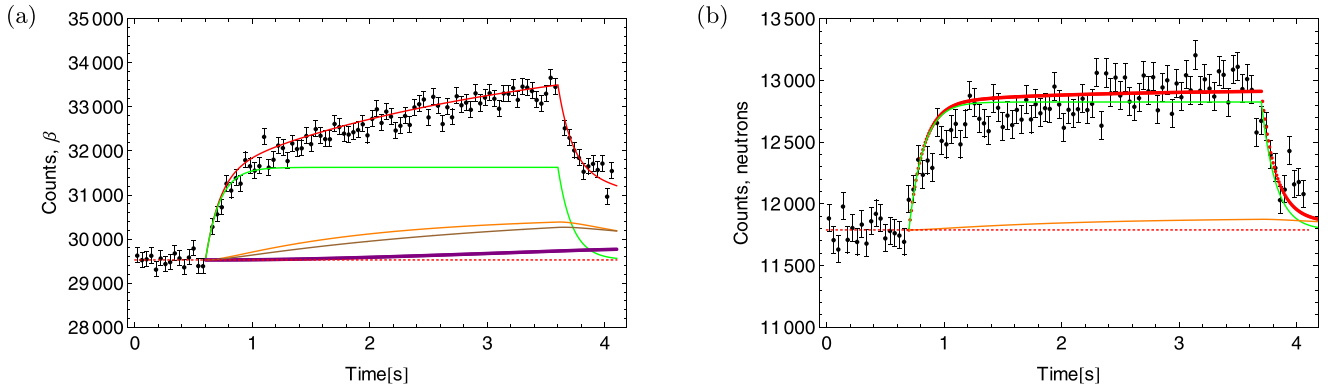


FIG. 7. β (a) and neutron (b) activity curves recorded for the $A = 84$ setting of the mass separator. These curves were accumulated over 17971 tape cycles. (a) The different β -activity components are singled out with colored curves: ^{84}Ga in green, ^{84}Ge in orange, ^{83}Ge in brown, ^{84}As in purple (^{83}As in cyan, almost identical to the previous one) and the background level is represented by the dotted line. (b) The two components of the β -delayed neutron activity curve originating from both ^{84}Ga (green) and ^{84}Ge (orange) decays are singled out.

may constitute the first experimental evidence for the emission of two neutrons following the β decay of ^{84}Ga . We note that this nucleus has long been predicted to be a β -delayed $2n$

precursor [40,41]. Further investigations on the possible β - $2n$ decay of ^{84}Ga , with higher statistics, will be necessary in order to be able to obtain a reliable P_{2n} value.

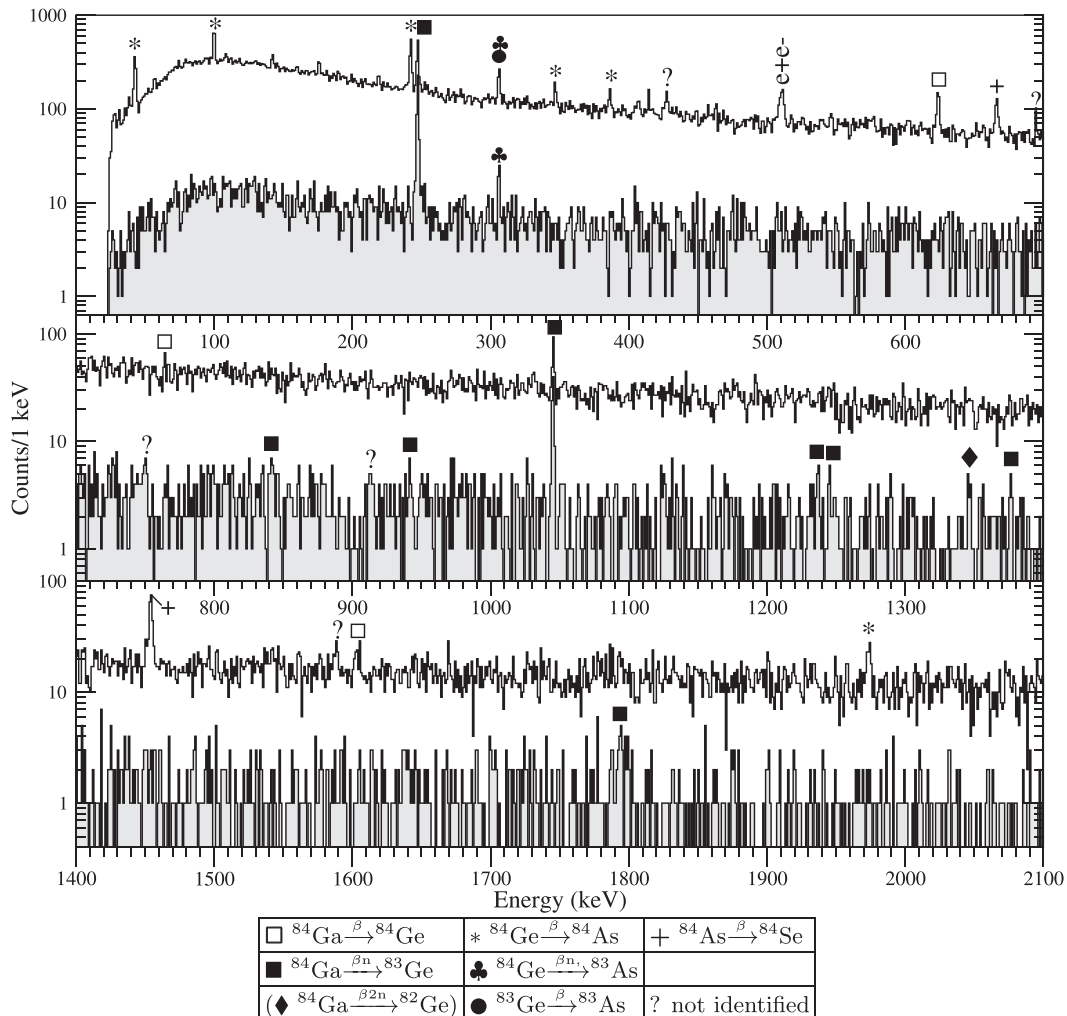


FIG. 8. β gated and β - n gated (shaded in gray) γ spectra recorded for the $A = 84$ setting of the mass separator.

TABLE VI. Photopeaks attributed to the β and β - n decays of ^{84}Ga identified in the spectra recorded for the $A = 84$ setting of the mass-separator. γ intensities are given relative to the one of the transition observed at 248 keV. All assignments are from Ref. [38] unless marked by an asterisk, in which cases the assignment is from the present work and additional explanation is provided in footnotes. Other quantities have the same meaning as in Table V.

E_γ [keV]	Spec	I_γ^{rel} [%]	$S_{\gamma\beta n}/S_{\gamma\beta}$	Assignment
248.1(4)	$\gamma\beta$	100(8)		$^{84}\text{Ga}(\beta n)$
	$\gamma\beta n$	100(7)	47(5)	
624.5(4)	$\gamma\beta$	65(8)		$^{84}\text{Ga}(\beta)$
	$\gamma\beta n$			
765.0(4)	$\gamma\beta$	18(6)		$^{84}\text{Ga}(\beta)$
	$\gamma\beta n$			
842.8(4)	$\gamma\beta$	17(7)		$^{84}\text{Ga}(\beta)n^{*a}$
	$\gamma\beta n$	22(5)	63(28)	
941.7(5)	$\gamma\beta$	12(8)		$^{84}\text{Ga}(\beta)n$
	$\gamma\beta n$	11(6)	43(35)	
1046.2(5)	$\gamma\beta$	56(9)		$^{84}\text{Ga}(\beta)n$
	$\gamma\beta n$	66(9)	56(11)	
1238.4(5)	$\gamma\beta$	12(8)		$^{84}\text{Ga}(\beta)n$
	$\gamma\beta n$	13(5)	52(42)	
1246.5(5)	$\gamma\beta$	^b		$^{84}\text{Ga}(\beta)n^{*c}$
	$\gamma\beta n$	9(4)		
1376.8(4)	$\gamma\beta$	15(9)		$^{84}\text{Ga}(\beta)n^{*a}$
	$\gamma\beta n$	15(4)	48(31)	
1603.9(5)	$\gamma\beta$	20(10)		$^{84}\text{Ga}(\beta)$
	$\gamma\beta n$			
1794.4(3)	$\gamma\beta$	25(10)		$^{84}\text{Ga}(\beta)n^{*a}$
	$\gamma\beta n$	22(7)	42(21)	

^aThis line was also present in the spectra of Ref. [38] but (wrongly) attributed to a contamination from neutron-rich Rb decays.

^bWeakest among the identifiable lines. The peak is visible but in a chaotic, large background region, for that reason the net count is below the critical limit for 95% confidence. However, it is well above this critical limit in the much cleaner βn -gated spectrum.

^cPoor energy agreement with the line observed at 1245.7 keV and recently attributed to the β decay of ^{83}Ga in Ref. [25] (probably due to note^b).

IV. DISCUSSION

As can be seen in Fig. 9 our results point toward a sizable ($N_m + 1, 2, 3$) P_{1n} oscillation for the Ga chain, with an amplitude exceeding by far what previous measurements, Fig. 2, could suggest. P_{1n} odd-even staggering is a very well-known phenomenon, attributed to pairing effects. However, the effect which is observed here considerably exceeds what can be expected from this trivial origin: This is illustrated by the results from the so-called gross theory, reported in Fig. 9, which exhibit only a change of the slope of the P_{1n} evolution.

1. Use of the McCutchan *et al.* empirical formula

It is informative now to compare also our results with the predictions of a new empirical P_{1n} formula introduced by McCutchan *et al.* [44] considering the $P_{1n}/T_{1/2}$ ratio as a (power) function of $Q_{\beta n}$ and an improved alternative to the Kratz-Hermann [45] formula. The use of this ratio comes

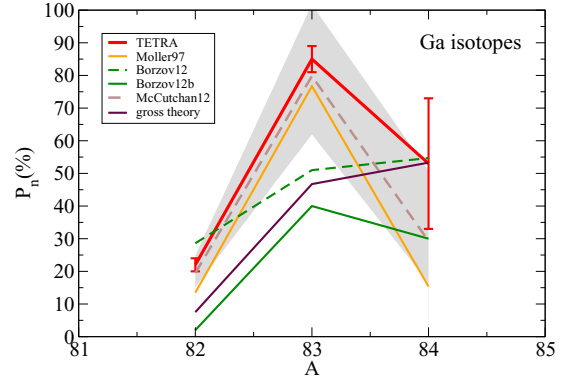


FIG. 9. Experimental P_{1n} for the $^{82-84}\text{Ga}$ precursors from the present work (“TETRA”) compared to theoretical results using QRPA approaches (“Moller97” from Ref. [40] and “Borzov12b,Borzov12” from Ref. [42], with and without blocking effects, respectively) or the gross theory for β decay [43]. Results from the use of the empirical formula by McCutchan *et al.* [44] (“McCutchan12”) are also represented with the associated uncertainties materialized by the gray zone.

from the basic, though previously unexploited recognition that it directly represents the integrated β strength available in the ($Q_\beta - S_n$) energy window [44]:

$$\frac{P_{1n}}{T_{1/2}} \propto \int_{S_n}^{Q_\beta} S_\beta(E) f(Z, Q_\beta - E) dE,$$

where $S_\beta(E)$ is the β -strength function and $f(Z, Q_\beta - E)$ is the Fermi integral. An interesting aspect of this new approach is that this quantity is free from the strong and strongly varying effects due to GT transitions to the low-lying (below S_n) part of the emitter energy spectrum.

In Fig. 9, we report the results given by the formula using (i) the fit parameters obtained in Ref. [44] for light fission fragments, (ii) the $^{82-84}\text{Ga}$ half-lives from our work, except for ^{84}Ga where the value of 84(7) ms from Ref. [38] was used, and (iii) evaluated [46] $Q_{\beta n}$ values. For $A = 82, 83$ the agreement between predictions from the formula and our results is impressive. In Ref. [47], Fig. 2, McCutchan *et al.* presented a systematics of the ratio $R = P_{1n}^{\text{exp}}/P_{1n}^{\text{theory}}$ (where P_{1n}^{theory} is their formula’s result) for the Ga isotopes. The only case where R was lower than 1 was ^{83}Ga . $R < 1$ means a too small P_{1n} or a too large $T_{1/2}$. Since consistent and precise values for ^{83}Ga half-life are now available (Refs. [17,25] and the present work) the problem necessarily came from an underestimated experimental P_{1n} . With our P_{1n} value, $R(^{83}\text{Ga})$ is brought back very close to unity.

Our uncertainties on the $P_{1n}(^{84}\text{Ga})$ determination are large, but it is seen that the central value is at the upper limit of the range of possible values computable using the empirical formula. This range of possible values, represented by the shaded region in Fig. 9, was obtained taking into account the uncertainties on all the quantities entering into the formula (e.g., the $Q_{\beta n}$ window is only an estimated extrapolation in the database [46]). The expected central value is $P_{1n} = 29\%$; our experimental value is compatible with it within $\approx 1\sigma$.

The conclusion which can be drawn from this extensive exploitation of the new empirical formula by McCutchan *et al.* must be clear at this point: The jump of the P_{1n} value observed for ^{83}Ga is simply due to a sudden increase of the β strength available in the $Q_{\beta n}$ window with respect to ^{82}Ga . While this effect is certainly in part a mechanical consequence of the natural increase of the window's size, it is also necessary that GT-fed states are present in the lowest part of the window. Moving from ^{83}Ga to ^{84}Ga , the fraction of the β strength present inside the $Q_{\beta n}$ window increases by only $\approx 1/3$ while the decay rate is increased by a factor ≈ 3.7 . This means that for ^{84}Ga a significant fraction of the β strength—and necessarily the lowest-energy part of it—now escapes the $Q_{\beta n}$ window, lying below S_n in the emitter ^{84}Ge , resulting in a reduced P_{1n} . This is exactly the same phenomenon that was invoked in Ref. [8] to explain the P_{1n} trend in the K isotopic chain (see Sec. I).

2. Comparison with QRPA results

The real question is now to know what could be the microscopic origin of these low-lying GT-fed states. Mean-field approaches, particularly including a treatment of correlations within the quasiparticle random-phase approximation (QRPA), are generally the best suited (and preferred) tools to investigate such a question. Calculations of β -decay properties using shell-model approaches are made difficult because of the large valence spaces, including several major shells, which are in principle needed. This is especially true for the region considered here, located near a major shell closure. Selected results from QRPA calculations are also reported in Fig. 9. The only calculation showing a P_{1n} oscillation for $^{82-84}\text{Ga}$, of amplitude similar to the one observed, that we could find in the literature is part of the global QRPA calculations performed by Möller *et al.* [40] 20 years ago. However, the same calculations completely fail to reproduce the P_{1n} sequence of the K isotopic chain represented in Fig. 1. More recent calculations by Borzov [42] including both a treatment of the first-forbidden β transitions and of blocking effects are also shown in Fig. 9. Calculations without blocking show a trend similar to the one from the gross theory, while the inclusion of blocking leads to a clear P_{1n} oscillation but with an amplitude much lower than the one observed experimentally.

3. A phenomenological attempt toward a detailed microscopic interpretation

In a further attempt to gain deeper insight into the microscopic nature of the low-lying GT-fed states possibly responsible for the observed phenomenon, we have considered the configurations and valence space shown in Fig. 10 in a phenomenological way. In this simplistic approach, the ground state of the precursor is assumed to be represented as a one proton quasiparticle (QP) j_{p0} state. GT transitions from this state to the neutron-hole proton-particle configurations coupled to $J^\pi = 1^+$ (“doorway configurations”) schematically represented in Fig. 10(a), with all possible combinations allowed by the valence space represented in Fig. 10(b), were considered.

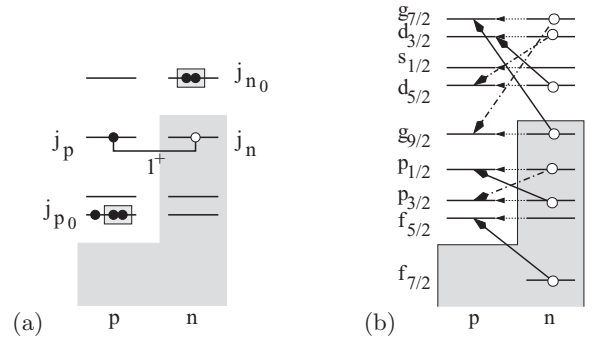


FIG. 10. (a) Schematic representation of a typical configuration fed by a single-particle GT transition. (b) Valence space and GT transitions considered in the calculation: full, dashed-dotted, and dotted arrows represent GT single-particle transitions to spin-flip, back spin-flip, and core-polarized states, respectively.

The unperturbed (effective single particle) energies of the doorway configurations were extracted from spectroscopic information on the $N = 49$ isotones within a core-coupling approach using the procedure of Ref. [34]. Configuration energy was calculated taking into account an effective residual proton-neutron interaction in the $J^\pi = 1^+$ channel derived from the observed splittings of the J^π multiplets in the odd-odd $N = 49$ nuclei, similar to what was done also in Ref. [34]. The low-lying 1^+ states in these nuclei involve indeed exactly the same neutron-hole proton-particle configurations as represented in Fig. 10. QP occupation coefficients were determined using a BCS approximation and pairing gaps from existing experimental mass data. However, in this voluntarily simplistic first approach, configuration mixing and phonon coupling were not included. Their inclusion would lead to two seemingly opposite effects, the former depriving the lowest lying states of their GT strength while shifting them to higher energy, while the latter introduces low-lying small GT-strength components. Only proper, detailed QRPA (or very large-scale shell-model) calculations can provide the correct balance.

We have tested our approach on the analogous case of the $N = 52$ ^{87}Br precursor to the $N = 51$ ^{87}Kr emitter β decay for which detailed experimental GT-strength distributions are available [48,49]. The resulting GT-strength function is shown in Fig. 11, and it is in good agreement with the one experimentally obtained; see Fig. 4 in Ref. [48] or Fig. 8 in Ref. [49]. In particular, the energy location and width of the resonance-like structure centered around 5.5 MeV are nicely reproduced. According to the calculations, it is centered around a dominant $\nu 1g_{9/2} \rightarrow \pi 1g_{9/2}$ CP component. This agreement means that the existence of this broad structure and its energy location are consistent with the rest of the observed lower-lying spectroscopy. The experimentally observed accumulation of strength just below Q_β is missed by the calculations, but this is probably simply due to the lack of configuration mixing, which could lead to an accumulation of strength on the (maybe also underestimated) $\nu 1f_{7/2} \rightarrow \pi 1f_{5/2}$ SF component.

Following these encouraging results, calculations were pursued for the $^{83}\text{Ga}_{52} \rightarrow ^{83}\text{Ge}_{51}\beta$ decay and the associated GT-strength distribution is reported in Fig. 12. The change in

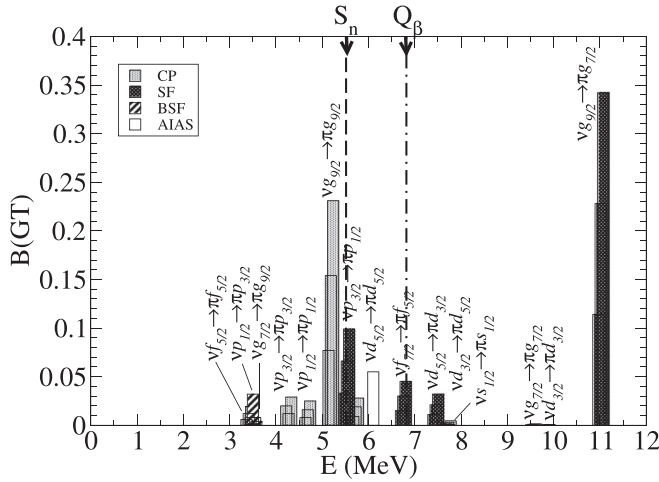


FIG. 11. GT probabilities [$B(\text{GT})$] of transitions from the ^{87}Br ground state (assumed as a proton $j_{p0} \equiv 2p_{3/2}$ QP state) to $J = 1/2, 3/2, 5/2$ components of the doorway configurations in the daughter ^{87}Kr . The different contributions to spin-flip (SF), back spin-flip (BSF), core-polarized (CP), and anti-isobaric analog (AIAS) states (following the nomenclature of Ref. [50]) are shown with different filling patterns. The neutron-hole proton-particle involved are explicitly given near the associated GT component. The vertical dotted and dashed-dotted lines indicate the position of the neutron threshold in the ^{87}Kr emitter and the Q_β of the ^{87}Br precursor, respectively.

the strength function from the previous heavier $N = 51$ case is not trivial. The 5.5-MeV-centered resonance-like structure is apparently still present, but is broadened and split into rather well-separated components collecting similar strength. Interestingly enough, the lowest one is formed by the rather strong BSF $v2p_{1/2} \rightarrow \pi2p_{3/2}$ transition, somewhat isolated from the rest of the structure. Its excitation energy is located

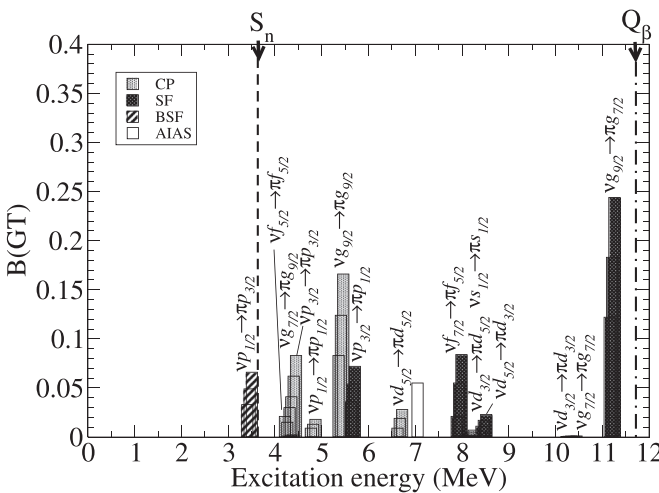


FIG. 12. Same as Fig. 11 but for the decay of the ^{83}Ga ground state, assumed as a proton $j_{p0} \equiv 1f_{5/2}$ QP state, to the $J = 3/2, 5/2, 7/2$ GT doorway states in ^{83}Ge . The vertical dotted and dashed-dotted lines indicate the position of the neutron threshold in the ^{83}Ge emitter and the Q_β of the ^{83}Ga precursor, respectively.

very near the neutron separation threshold (inclusion of configuration mixing would push it just above). It seems then that it is indeed due to this particular structure in the lowest part of the GT-strength distribution that P_{1n} reduction is observed when going from ^{83}Ga to ^{84}Ga . The neutron separation threshold increases from 3633(3) keV in ^{83}Ge to 5243(4) keV ^{84}Ge [46], thus suddenly excluding this specific BSF component (and maybe also part of the CP components) from the Q_β window. This effect is magnified by the Fermi function: This sole BSF configuration attracts already $\lesssim 27\%$ (at maximum) of the β population.

Neutrons emitted from these states must have a very small energy, leaving the n -emitted residue ^{82}Ge in its ground state. But one of the characteristics of the TETRA ^3He neutron counter is precisely to have a negligible neutron-energy threshold [22]. Incidentally, we report 20(8)% γ -unobserved βn feeding (see Table IV), which compares favorably with the $\lesssim 27\%$ feeding to the BSF states. It is worth pointing out that it is also consistent with the $\approx 30\%$ missing βn strength in the measurement of Ref. [14].

In conclusion, this phenomenological study, while having the clear advantage to allow for a simple picture in terms of the single-particle states involved, provides strong additional support to the conclusion drawn from the use of the empirical P_{1n} formula.

V. CONCLUSION

β -delayed neutron emission probabilities of the $^{82-84}\text{Ga}$ precursors were measured in simultaneous β and neutron counting mode using the 4π long-counter TETRA at the ALTO ISOL facility. Detailed β and neutron-gated γ -spectroscopy data were collected. First experimental evidence for β -delayed two-neutrons emission from the ^{84}Ga precursor was also found. $P_{1n} = 22(2), 85(4)$, and $53(20)\%$ were obtained for ^{82}Ga , ^{83}Ga , and ^{84}Ga respectively. The P_{1n} extraction procedure was validated on the ^{82}Ga case [22] and further improvements were introduced in the present work for the case of ^{83}Ga , where statistics was sufficient to extract one P_{1n} value per individual tape cycle, thus dramatically improving the statistical significance of the final result.

The trend which emerges from this set of three values is that of a large amplitude P_{1n} staggering. The decrease of the P_{1n} value from ^{83}Ga to ^{84}Ga recently pointed out in Ref. [14] is confirmed but is even more dramatic, starting from a much higher P_{1n} value for ^{83}Ga than reported before. Such a large P_{1n} oscillation for neutron precursors having a magic number N_m of neutrons +1, 2, and 3 additional ones was already observed in the case of the K isotopes beyond the $N_m = 28$ shell closure by Carraz *et al.* [8]. This phenomenon was interpreted by these authors as originating from low-lying structures in the β -strength function. An analysis using the new empirical P_{1n} formula recently introduced by McCutchan *et al.* [44] supports a same interpretation for the present case. Further investigation on possible GT doorway configurations available at low energy according to the $N = 49$ spectroscopy points toward the presence of a strongly fed proton-particle neutron-hole [$\pi2p_{3/2}^1 v2p_{1/2}^{-1} 1_+$ \otimes $\pi2f_{5/2}$ back-spin-flip configuration located exactly in the region of the neutron threshold.

By its magnitude, this $(N_m + 1, 2, 3)$ P_{1n} -staggering phenomenon seems to bear some characteristics of a resonant process and may belong to a wider class of nuclear threshold phenomena. In any case, it is most probably not a simple curiosity restricted to the K or Ga cases. It may indeed explain the anomalies of the effective density parameters of structureless β -strength functions in an attempt to fit to the whole set of experimentally available P_{1n} value, as in Ref. [13]. Further investigation in the $N_m = 82$ region, in particular “south” of ^{132}Sn , would provide valuable clues about the possible generality of this $(N_m + 1, 2, 3)$ P_{1n} -staggering phenomenon.

While it is in general difficult to exploit integrated quantities like P_{1n} (or half-lives, masses, etc.) for nuclear structure purposes, their measurements for a series of $(N_m + 1, 2, 3)$ nuclei can really be hoped to bring new insights on the structure of the closed (or supposedly closed) shell regions in question. These integrated quantities are in general the first available for very exotic nuclei, because their measurements are achieved

using high-sensitivity or high-efficiency detectors. In those conditions, they can be truly viewed as a first step towards spectroscopy—viz., in the case of systematic P_{1n} measurements, towards spectroscopic studies of the neutron-threshold region of the excitation spectrum.

ACKNOWLEDGMENTS

We thank the technical staff of the Tandem/ALTO facility for their assistance in the experiment and for smooth operation of the e-LINAC and PARRNe mass separator. The authors wish to acknowledge support from the bilateral agreement JINR-CNRS/IN2P3 No. 06-75, from the Joint Research Project (PRC) between CNRS and the Russian Foundation for Basic Research, Grant No. PRC 6336 and from the Russian Foundation for Basic Research, Grant No. 14-02-91053CNRSa. H.P. is thankful for the hospitality of IPN-Orsay during his internship. The use of one Ge detector from the French-UK IN2P3-STFC Gamma Loan Pool is acknowledged.

-
- [1] J. Hardy, B. Jonson, and P. Hansen, *Nucl. Phys. A* **305**, 15 (1978).
- [2] S. Prussin, Z. Oliveira, and K.-L. Kratz, *Nucl. Phys. A* **321**, 396 (1979).
- [3] F. M. Mann, C. Dunn, and R. E. Schenter, *Phys. Rev. C* **25**, 524 (1982).
- [4] K.-L. Kratz, *Nucl. Phys. A* **417**, 447 (1984).
- [5] K.-L. Kratz, L. Alquist, G. I. Crawford, H. Gabelmann, G. Jung, H. V. Klapdor-Kleingrothaus, J. Metzinger, T. Oda, H. Ohm, B. Pfeiffer, A. Schröder, and W. Ziegert, in *Proceedings of the Fourth International Conference on Nuclei far from Stability*, edited by P. G. Hansen and O. B. Nielsen (CERN Yellow Report 81-09, Geneva, 1981), pp. 317–326.
- [6] H. V. Klapdor, T. Oda, J. Metzinger, W. Hillebrandt, and F. K. Thielemann, *Z. Phys. A: At. Nucl.* **299**, 213 (1981).
- [7] H. Ejiri, K. Ikeda, and J.-I. Fujita, *Phys. Rev.* **176**, 1277 (1968).
- [8] L. Carraz, P. Hansen, A. Huck, B. Jonson, G. Klotz, A. Knipper, K. Kratz, C. Miéché, S. Mattsson, G. Nyman, H. Ohm, A. Poskanzer, A. Poves, H. Ravn, C. Richard-Serre, A. Schröder, G. Walter, and W. Ziegert, *Phys. Lett. B* **109**, 419 (1982).
- [9] T. Burrows, *Nucl. Data Sheets* **107**, 1747 (2006).
- [10] T. Burrows, *Nucl. Data Sheets* **109**, 1879 (2008).
- [11] Z. Elekes, J. Timar, and B. Singh, *Nucl. Data Sheets* **112**, 1 (2011).
- [12] H. Xiaolong, *Nucl. Data Sheets* **107**, 2131 (2006).
- [13] K. Miernik, *Phys. Rev. C* **88**, 041301 (2013).
- [14] M. Madurga, S. V. Paulauskas, R. Grzywacz, D. Miller, D. W. Bardayan, J. C. Batchelder, N. T. Brewer, J. A. Cizewski, A. Fijałkowska, C. J. Gross, M. E. Howard, S. V. Ilyushkin, B. Manning, M. Matoš, A. J. Mendez, K. Miernik, S. W. Padgett, W. A. Peters, B. C. Rasco, A. Ratkiewicz, K. P. Rykaczewski, D. W. Stracener, E. H. Wang, M. Wolińska-Cichocka, and E. F. Zganjar, *Phys. Rev. Lett.* **117**, 092502 (2016).
- [15] E. Lund, P. Hoff, K. Aleklett, O. Glomset, and G. Rudstam, *Z. Phys. A: At. Nucl.* **294**, 233 (1980).
- [16] R. A. Warner and P. L. Reeder, *Radiat. Eff.* **94**, 27 (1986).
- [17] K. L. Kratz, H. Gabelmann, P. Möller, B. Pfeiffer, H. L. Ravn, and A. Wöhr, *Z. Phys. A: Hadrons Nucl.* **340**, 419 (1991).
- [18] G. Rudstam, K. Aleklett, and L. Sihver, *At. Data Nucl. Data Tables* **53**, 1 (1993).
- [19] C. Gross, J. Winger, S. Ilyushkin, K. Rykaczewski, S. Liddick, I. Darby, R. Grzywacz, C. Bingham, D. Shapira, C. Mazzocchi *et al.*, *Acta Phys. Pol. B* **40**, 447 (2009).
- [20] J. A. Winger, K. P. Rykaczewski, C. J. Gross, R. Grzywacz, J. C. Batchelder, C. Goodin, J. H. Hamilton, S. V. Ilyushkin, A. Korgul, W. Królas, S. N. Liddick, C. Mazzocchi, S. Padgett, A. Piechaczek, M. M. Rajabali, D. Shapira, E. F. Zganjar, and J. Dobaczewski, *Phys. Rev. C* **81**, 044303 (2010).
- [21] D. Testov, E. Kuznetsova, and J. Wilson, *J. Instrum.* **10**, P09011 (2015).
- [22] D. Testov, D. Verney, B. Roussière, J. Bettane, F. Didierjean, K. Flanagan, S. Franchoo, F. Ibrahim, E. Kuznetsova, R. Li, B. Marsh, I. Matea, Y. Penionzhkevich, H. Pai, V. Smirnov, E. Sokol, I. Stefan, D. Suzuki, and J. Wilson, *Nucl. Instrum. Methods Phys. Res., Sect. A* **815**, 96 (2016).
- [23] S. Essabaa, N. Barré-Boscher, M. C. Mhamed, E. Cottureau, S. Franchoo, F. Ibrahim, C. Lau, B. Roussière, A. Saïd, S. Tusseau-Nenez, and D. Verney, *Nucl. Instrum. Methods Phys. Res., Sect. B* **317**, 218 (2013).
- [24] E. McCutchan, *Nucl. Data Sheets* **125**, 201 (2015).
- [25] M. F. Alshudifat, R. Grzywacz, M. Madurga, C. J. Gross, K. P. Rykaczewski, J. C. Batchelder, C. Bingham, I. N. Borzov, N. T. Brewer, L. Cartegni, A. Fijałkowska, J. H. Hamilton, J. K. Hwang, S. V. Ilyushkin, C. Jost, M. Karny, A. Korgul, W. Królas, S. H. Liu, C. Mazzocchi, A. J. Mendez, K. Miernik, D. Miller, S. W. Padgett, S. V. Paulauskas, A. V. Ramayya, D. W. Stracener, R. Surman, J. A. Winger, M. Wolińska-Cichocka, and E. F. Zganjar, *Phys. Rev. C* **93**, 044325 (2016).
- [26] J. Tuli, *Nucl. Data Sheets* **98**, 209 (2003).
- [27] J. K. Hwang, J. H. Hamilton, A. V. Ramayya, N. T. Brewer, Y. X. Luo, J. O. Rasmussen, and S. J. Zhu, *Phys. Rev. C* **84**, 024305 (2011).
- [28] L. A. Currie, *Anal. Chem.* **40**, 586 (1968).

- [29] G. Gilmore and J. D. Hemingway, *Practical γ -Ray Spectrometry* (Wiley, New York, 1995).
- [30] D. Testov, Effect of shell closures $N = 50$ and $N = 82$ on the structure of very neutron-rich nuclei produced at ALTO. Measurements of neutron emission probabilities and half lives of nuclei at astrophysical r-process path, Ph.D. thesis, Université Paris Sud, Orsay, France, 2014; internal report IPNO-T-13-07 (unpublished).
- [31] O. Perru, Etude des fermetures de couches $N = 40$ et $N = 50$ dans les noyaux riches en neutrons, Ph.D. thesis, Université Paris Sud, Orsay, France, 2004; internal report IPNO-T-05-02 (unpublished).
- [32] P. Hoff and B. Fogelberg, *Nucl. Phys. A* **368**, 210 (1981).
- [33] K. Miernik, K. P. Rykaczewski, C. J. Gross, R. Grzywacz, M. Madurga, D. Miller, J. C. Batchelder, N. T. Brewer, C. U. Jost, K. Kolos, A. Korgul, C. Mazzocchi, A. J. Mendez, Y. Liu, S. V. Paulauskas, D. W. Stracener, J. A. Winger, M. Wolińska-Cichocka, and E. F. Zganjar, *Phys. Rev. C* **90**, 034311 (2014).
- [34] A. Etilé, D. Verney, N. N. Arsenyev, J. Bettane, I. N. Borzov, M. Cheikh Mhamed, P. V. Cuong, C. Delafosse, F. Didierjean, C. Gaulard, N. Van Giai, A. Goasduff, F. Ibrahim, K. Kolos, C. Lau, M. Niikura, S. Roccia, A. P. Severyukhin, D. Testov, S. Tusseau-Nenez, and V. V. Voronov, *Phys. Rev. C* **91**, 064317 (2015).
- [35] A. Gottardo, D. Verney, I. Deloncle *et al.* (unpublished).
- [36] C. Delafosse, D. Verney *et al.* (unpublished).
- [37] D. Abriola, M. Bostan, S. Erturk, M. Fadil, M. Galan, S. Juutinen, T. Kibédi, F. Kondev, A. Luca, A. Negret, N. Nica, B. Pfeiffer, B. Singh, A. Sonzogni, J. Timar, J. Tuli, T. Venkova, and K. Zuber, *Nucl. Data Sheets* **110**, 2815 (2009).
- [38] K. Kolos, D. Verney, F. Ibrahim, F. Le Blanc, S. Franchoo, K. Sieja, F. Nowacki, C. Bonnin, M. Cheikh Mhamed, P. V. Cuong, F. Didierjean, G. Duchêne, S. Essabaa, G. Germogli, L. H. Khiem, C. Lau, I. Matea, M. Niikura, B. Roussière, I. Stefan, D. Testov, and J.-C. Thomas, *Phys. Rev. C* **88**, 047301 (2013).
- [39] A. Korgul, K. P. Rykaczewski, R. K. Grzywacz, C. R. Bingham, N. T. Brewer, C. J. Gross, A. A. Ciemny, C. Jost, M. Karny, M. Madurga, C. Mazzocchi, A. J. Mendez, K. Miernik, D. Miller, S. Padgett, S. V. Paulauskas, M. Piersa, D. W. Stracener, M. Stryjczyk, M. Wolińska-Cichocka, and E. F. Zganjar, *Phys. Rev. C* **93**, 064324 (2016).
- [40] P. Möller, J. Nix, and K.-L. Kratz, *At. Data Nucl. Data Tables* **66**, 131 (1997).
- [41] P. Möller, B. Pfeiffer, and K.-L. Kratz, *Phys. Rev. C* **67**, 055802 (2003).
- [42] I. N. Borzov, *EPJ Web Conf.* **38**, 12002 (2012).
- [43] T. Tachibana and M. Yamada, Estimation of β -decay properties [<http://www.wndc.jaea.go.jp/nuclldata/>].
- [44] E. A. McCutchan, A. A. Sonzogni, T. D. Johnson, D. Abriola, M. Birch, and B. Singh, *Phys. Rev. C* **86**, 041305 (2012).
- [45] K. L. Kratz and G. Herrmann, *Z. Phys.* **263**, 435 (1973).
- [46] G. Audi, F. Kondev, M. Wang, B. Pfeiffer, X. Sun, J. Blachot, and M. MacCormick, *Chin. Phys. C* **36**, 1157 (2012).
- [47] E. McCutchan, A. Sonzogni, T. Johnson, D. Abriola, M. Birch, and B. Singh, *Nucl. Data Sheets* **120**, 62 (2014).
- [48] F. Nuh, D. Slaughter, S. Prussin, H. Ohm, W. Rudolph, and K.-L. Kratz, *Nucl. Phys. A* **293**, 410 (1977).
- [49] S. Raman, B. Fogelberg, J. A. Harvey, R. L. Macklin, P. H. Stelson, A. Schröder, and K. L. Kratz, *Phys. Rev. C* **28**, 602 (1983).
- [50] H. Klapdor, J. Metzinger, and T. Oda, *At. Data Nucl. Data Tables* **31**, 81 (1984).